The EMBO Journal Vol.17 No.15 pp.4238–4248, 1998

Response regulator output in bacterial chemotaxis

Uri Alon[1,2], Laura Camarena[3], Michael G.Surette[4], Blaise Aguera y Arcas[1], Yi Liu[1], Stanislas Leibler[1,2] and Jeffry B.Stock[1,5,6]

[1]Department of Molecular Biology, [2]Department of Physics, [5]Department of Chemistry, Princeton University, Princeton, NJ 08544, USA, [3]Department of Molecular Biology, Instituto de Investigation Biomedicas, UNAM, Apartado Postal 70-228 04510, Mexico D.F., Mexico and [4]Department of Microbiology and Infectious Diseases, University of Calgary, Calgary, AB, Canada T2N 4N1

[6]Corresponding author

Chemotaxis responses in *Escherichia coli* are mediated by the phosphorylated response-regulator protein P-CheY. Biochemical and genetic studies have established the mechanisms by which the various components of the chemotaxis system, the membrane receptors and Che proteins function to modulate levels of CheY phosphorylation. Detailed models have been formulated to explain chemotaxis sensing in quantitative terms; however, the models cannot be adequately tested without knowledge of the quantitative relationship between P-CheY and bacterial swimming behavior. A computerized image analysis system was developed to collect extensive statistics on free-swimming and individual tethered cells. P-CheY levels were systematically varied by controlled expression of CheY in an *E.coli* strain lacking the CheY phosphatase, CheZ, and the receptor demethylating enzyme CheB. Tumbling frequency was found to vary with P-CheY concentration in a weakly sigmoidal fashion (apparent Hill coefficient ~2.5). This indicates that the high sensitivity of the chemotaxis system is not derived from highly cooperative interactions between P-CheY and the flagellar motor, but rather depends on nonlinear effects within the chemotaxis signal transduction network. The complex relationship between single flagella rotation and free-swimming behavior was examined; our results indicate that there is an additional level of information processing associated with interactions between the individual flagella. An allosteric model of the motor switching process is proposed which gives a good fit to the observed switching induced by P-CheY. Thus the level of intracellular P-CheY can be estimated from behavior determinations: ~30% of the intracellular pool of CheY appears to be phosphorylated in fully adapted wild-type cells.

Keywords: bacterial swimming/*Escherichia coli*/image analysis/P-CheY

Introduction

Bacteria such as *E.coli* swim by rotating several flagella (for a recent review of *E.coli* motility see Macnab, 1996). Each flagellum is attached to the cell at a complex basal body apparatus that functions as a bi-directional rotary motor. Rotating flagella filaments coalesce into a bundle that pushes the cell body in a curvilinear trajectory termed a 'run'. Runs are interrupted when the flagella fly apart and the cell tumbles in place, randomizing the direction of the subsequent run. By modulating the frequency of tumbles, the bacteria are able to perform chemotaxis, achieving a net motion towards attractants and away from repellants (Berg and Brown, 1972). The motion of individual motors can be visualized by tethering a flagellum to a coverslip and viewing the rotation of the cell body. From such experiments it has been determined that there is a general correlation of running behavior with counterclockwise (CCW) motor rotation, and a correlation of tumbling behavior with clockwise (CW) motor rotation (Larsen *et al.*, 1974).

Escherichia coli regulate their tumbling frequency through the activity of the Che proteins, which form a signal transduction network (for recent reviews see Eisenbach, 1996; Stock and Surette, 1996; Falke *et al*., 1997). This network interacts with the motor via the response regulator protein CheY. CheY is phosphorylated by the kinase CheA, and CheA kinase activity is regulated by the transmembrane chemotaxis receptors. P-CheY is dephosphorylated by the phosphatase CheZ. Genetic and biochemical studies indicate that P-CheY binds to the motor and promotes CW rotation. Thus, for instance, mutant strains that are deficient in CheA or CheY tend to run continually whereas mutants deficient in CheZ are highly tumbly. Increases in attractant concentration inhibit kinase activity, leading to reduced levels of P-CheY and suppression of tumbling. Thus, when a cell runs up an attractant gradient it tends to continue in that direction. The chemotaxis signal transduction system has been extensively studied under defined conditions with purified components, and models based on these results have been formulated to explain in quantitative terms the effects of various mutations and stimuli on the levels of P-CheY (Segel *et al*., 1986; Bray *et al.*, 1993; Bray and Bourret, 1995; Hauri and Ross, 1995; Barkai and Leibler, 1997; Spiro *et al.*, 1997). The strength of this approach would be significantly augmented if a direct quantitative relationship between the *in vivo* level of P-CheY and swimming behavior were known. In this report we have attempted to determine this relationship.

Because of the inherent chemical instability of the aspartyl phosphate in P-CheY, it is not feasible to measure directly the fraction of CheY phosphorylated in the cell. Previous studies of the effect of CheY on cell behavior were performed using strains with undefined kinase activity (Kuo and Koshland, 1987, 1989), so the equivalent level of wild-type P-CheY could not be estimated. To bypass these problems, we have constructed a mutant

strain that lacks both the P-CheY phosphatase, CheZ, and the downregulator of kinase activity, CheB. Several lines of evidence indicate that in this strain essentially all the CheY present is phosphorylated. Variable levels of CheY were expressed in this background from a low-copy plasmid with a regulated *lac* promoter, and CheY was quantitated by standard immunological techniques. Tethered-cell and swimming-cell assays were employed in parallel to establish a quantitative relation between behavior and P-CheY levels. Computerized image analysis (Sager *et al.*, 1988; Khan *et al.*, 1992; Amsler, 1996) was used to acquire extensive statistics in both assays. Both the tumbling frequency of swimming cells and the CW bias of tethered motors increase with increasing P-CheY concentration. However, the relationship between tethered-motor rotation and swimming behavior was not simple. Most of the differences could be ascribed to interactions between flagella that can be viewed as an additional level of information processing in the chemotaxis system. Comparing the behavior of wild-type cells with that induced by known amounts of P-CheY indicates that ~30% of CheY is phosphorylated in adapted wild-type cells. The relation between P-CheY and tumbling frequency also allowed us to compare the *in vivo* function of several CheY mutants with that of wild-type P-CheY. Our results suggest that *in vivo*, the constitutively active mutant CheYD13K is quantitatively equivalent to P-CheY. This complements a recent study in which motor rotation was related to the intracellular concentration of a similar activated CheY mutant (Scharf *et al.*, 1998).

The tumbling frequency of swimming cells exhibited only a weakly sigmoidal dependence on P-CheY (apparent Hill coefficient ~2.5). This result has important implications concerning our current understanding of the chemotaxis signal transduction system. Simulations based on the known biochemistry of the chemotaxis system indicate that the high sensitivity that cells exhibit to attractant stimuli (Berg and Brown, 1972; Segall *et al.*, 1986; Khan *et al.*, 1993) implies a highly cooperative interaction between P-CheY and the motor [with apparent Hill coefficients ranging from 8 to 11 (Ninfa *et al.*, 1991; Spiro *et al.*, 1997)]. The observation that this interaction is not highly cooperative suggests that the sensitivity of the chemotaxis system is due to some hitherto undefined molecular interaction within the signal transduction network that controls the level of CheY phosphorylation.

Results

Strategy for measuring behavior as a function of P-CheY

Escherichia coli strain PS2001, a derivative of the chemotaxis wild-type strain RP437 with a deletion from the beginning of *cheB* through *cheY* to the end of *cheZ*, was transformed with the low-copy-number plasmid pLC576 in which cheY is under control of the *lac* promoter (Table I). Production of CheY was controlled by varying the concentration of isopropyl-β-D-thiogalactoside (IPTG). In this strain, lack of CheB leads to full methylation of the chemoreceptors, and thus to a high activity of the kinase, CheA, which phosphorylates CheY. In addition, CheZ is missing, greatly reducing the rate of CheY dephosphorylation. Thus, in this strain virtually all of the CheY expressed is expected to be phosphorylated. This is supported by three lines of evidence. (i) From *in vitro* measurements of CheY phosphorylation by highly methylated receptor-CheA complexes, and of P-CheY dephosphorylation in the absence of CheZ, one would predict that >99.9% of CheY is maintained in a phosphorylated state in PS2001–pLC576 (Table II). From these calculations, even if the *in vivo* rate of CheY phosphorylation were 100-fold lower than the *in vitro* estimates, >90% of CheY would still be phosphorylated in this strain. (ii) The tumbling frequency of RP1616, a strain deleted for CheZ, is the same as the tumbling frequency of PS2001–pLC576 with CheY induced to wild-type level. (iii) The tumbling behavior of PS2001–pLC576 was not affected by addition of repellents (50 mM L-leucine or 100 μM indole, at various levels of CheY induction; data not shown). Thus, repellents can not further increase the P-CheY levels in this strain, consistent with phosphorylation of essentially all of CheY.

Cultures of PS2001–pLC576 grown in the presence of varying concentrations of the inducer IPTG were harvested at mid-log phase and the rotation of single tethered cells as well as the behavior of free-swimming cells was analyzed. Cells from each culture were also pelleted and frozen for subsequent quantitation of CheY by Western blot determinations. CheY expression increased with IPTG concentration from a basal level of ~700 CheY/cell in the absence of IPTG to ~35 000 CheY/cell in cells grown in 50 μM IPTG (Figure 1, inset). The total protein per cell, as well as the number of flagella per cell (6.7 ± 0.5, mean and SE for 25 cells), did not measurably vary with CheY expression.

Tethered cells

To measure the rotation of single flagellar motors, cells were tethered to coverslips coated with anti-flagella antiserum and analyzed by computerized image-processing. The analysis included all rotating cells in a field of view according to uniform criteria, eliminating any bias introduced by manual cell selection procedures. From the angular velocity trace for each cell, switches between CCW and CW motion were determined. Each cell typically displayed approximately the same absolute angular velocity in both CW and CCW states. The average fraction of time spent turning CW, f_{CW}, increased with increasing CheY concentration with an apparent Hill coefficient of 3.5 ± 1.0 (Figure 1). The switching process was further characterized by the mean duration of CW and CCW intervals (Figure 2). As expected, the mean CW duration increased and the mean CCW duration decreased with increasing P-CheY concentration. These results are similar to those of Kuo and Koshland (1989) who measured the effects of CheY expression in a strain that contained an incomplete deletion from *cheA* to *cheZ* that produces a fragment of CheA that is not subject to receptor activation. Because of the kinase deficiency, one might assume that relatively low levels of P-CheY were present in these experiments. Our results indicate that, in fact, a large fraction of the CheY must have been phosphorylated in these cells. A kinetic analysis based on *in vitro* rate estimates is consistent with this interpretation (Table II). A recent study showed a similar dependence of motor rotation on the level of an activated CheY mutant (Scharf

Table I. Strains and plasmids

	Comment	Source
Strain		
RP437	wild-type for chemotaxis, *lacY*$^-$, *ara*$^-$	J.S.Parkinson
PS2001	Δ*cheBcheYcheZ*	this study
PS2002	Δ*cheA–cheZ*, 'gutted strain'	this study
RP1616	Δ*cheZ*	J.S.Parkinson
Plasmid		
pHSG576	low copy, Cm^R	Takeshita *et al.* (1987)
pLC576	low copy, *cheY* under *lac* promoter, Cm^R	this study
pMS164	low copy, *cheYD13K* under *lac* promoter, Cm^R	this study
pMS168	medium copy, *cheYD57A* under *araBAD* promoter, Amp^R	this study

Table II. Estimates of fraction of CheY phosphorylated in various strains, based on *in vitro* rate constants

Strain	Kinase CheA autophosphorylation activity, k_A (s^{-1})	Fraction of CheY phosphorylated
PS2001–pLC576	20	0.9995
RP1616 (Δ*cheZ*)	13	0.9990
Kuo and Koshland (1987, 1989)	0.1	0.5–0.9

The relevant reactions are: CheA + MgATP – k_A → P-CheA + MgADP; P-CheA + CheY ← K_D → P-CheA–CheY – k_{trans} → CheA + P-CheY; and P-CheY – k_Y → CheY + P_i. The fraction of CheY phosphorylated was calculated from the steady state equation: $k_Y \times [\text{P-CheY}] = k_A[\text{CheA}]([\text{CheY}]_{total} - [\text{P-CheY}])/([\text{CheY}]_{total} - [\text{P-CheY}] + K_D)$. Measurements with purified components indicate that the equilibrium dissociation constant for CheY binding to P-CheA, K_D, is ~2 μM (Li *et al*., 1995; Shukla and Matsumura, 1995), the phosphotransfer reaction from P-CheA to CheY is not rate-limiting (k_{trans} >600/s; Stewart, 1997), and the rate of P-CheY dephosphorylation in the absence of CheZ is relatively slow, k_Y ~0.04/s (Hess *et al*., 1988; Lukat *et al*., 1991). Estimated rate constants for CheA autophosphorylation at saturating MgATP, k_A, in PS2001–pLC576 and in RP1616 correspond to values measured for CheA in complexes with CheW and the fully modified (all Q) or half modified (QEQE) receptor signaling domains, respectively (Borkovich *et al*., 1992; Liu *et al*., 1997). The strain used by Kuo and Koshland (1989) expressed a CheA–CheZ fusion that is not subject to receptor activation. The value of k_A in the Kuo and Koshland experiments is thus assumed to correspond to that of pure CheA in the absence of receptor (Tawa and Stewart, 1994; Surette and Stock, 1996). The level of CheA in *E.coli* has been estimated to be ~5 μM (Wang and Matsumura, 1997). The calculated values for fraction of CheY phosphorylated are essentially constant over the range of total CheY concentrations used in these studies (<100 μM) in the case of PS2001–pLC576 and RP1616, but with the much lower kinase activity in the strain used by Kuo and Koshland the fraction of CheY phosphorylated is expected to vary with total CheY as indicated.

et al., 1998; Figure 1). This indicates that the mutant has approximately the same activity as P-CheY.

Motor behavior displays significant variations from cell to cell (Berg and Tedesco, 1975; Spudich and Koshland, 1976; Ishihara *et al.*, 1983; Eisenbach *et al.*, 1990; Levin *et al*., 1998). We found that in PS2001–pLC576, at levels of CheY induction that caused approximately wild-type motor bias, a distribution of behaviors similar to wild-type was observed (Figure 3). This suggests that the plasmid system used in the present study does not introduce fluctuations between cells larger than those found naturally.

Swimming cells

Swimming behavior of cells was determined using the same cultures that were used to analyze the rotation of tethered motors. Cells were placed between a glass slide and a cover slip in a thin fluid layer of ~10 μm thickness. Their motion was observed by dark-field microscopy and recorded on videotape. The cells remained in the focal plane of the microscope at all times. The videotapes were analyzed by a computerized image analysis method developed to acquire extensive statistics on various aspects of swimming behavior. As expected, in the absence of CheY no tumbles were observed and cells tumbled with increasing frequency as P-CheY increased (Figure 4A–C). At very high levels of induction, however, the cells actually became less tumbly (Figure 4D). At low CheY concentrations, the tumble frequency increased in a weakly sigmoidal fashion with an apparent Hill coefficient of 2.5 ± 1 (Figure 5). The maximal degree of tumbling, 1.8 ± 0.1 tumbles/s, was observed at CheY concentrations of ~50 μM. At higher CheY concentrations, cells tumbled less, dropping to ~1.4 tumbles/s at 100 μM CheY. It seems probable that this decrease in tumbling frequency at CheY concentrations >50 μM is due to runs caused by the formation of CW rotating rather than CCW rotating flagella bundles (Wolf and Berg, 1989). The existence of such CW bundles and their ability to support runs has previously been demonstrated in strains with mutations that lock the motor in a CW state (Khan *et al.*, 1978). The average run speed decreased slightly with increasing CheY levels (Figure 6), with a rather sharp drop to ~50% of the maximal run speed at CheY concentrations >50 μM. The initial gentle decrease in run speed with increasing tumbling frequency is probably due to the fact that the cell speed takes a certain amount of time to recover from each tumble (Berg and Brown, 1972).

We also measured the duration of run and tumble events. The mean run duration decreased with increasing CheY concentration until a minimum was reached at a CheY concentration of ~50 μM (Figure 7B). In contrast, the duration of tumbling intervals remained approximately constant at 0.20 ± 0.05 s over the entire range of CheY induction (Figure 7A).

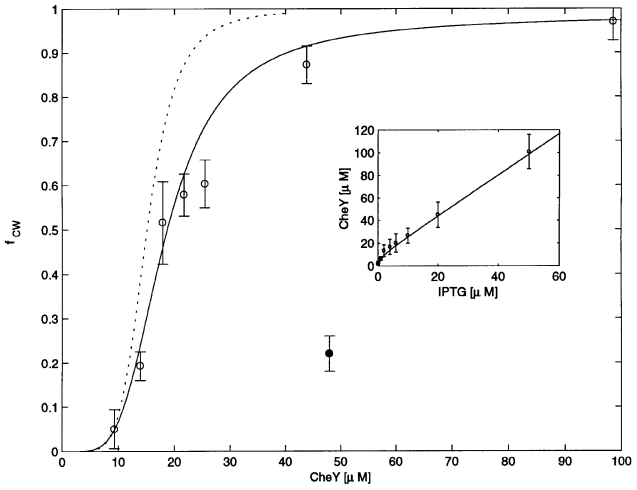

Fig. 1. Fraction of time tethered cells spend turning CW (f_{CW}). Cells induced with various amounts of IPTG were tethered and their motion was analyzed using video tracking. Each point is an average of data from 15–40 different tethered cells, analyzed for 100 s each. Open circles, strain PS2001–pLC576; solid circle, wild-type strain RP437–pHSG576. Error bars correspond to standard error of the mean. Solid line, fit to the allosteric model (see Discussion). The model parameters are: N = 30 binding sites for P-CheY, allosteric constant of $L_0 = 10^7$, dissociation constant for P-CheY binding K = 7.6 μM and ratio of binding affinity to CW and CCW states Ψ = 2.0. Dashed line, allosteric model with K = 12.5 μM and Ψ = 2.3, a best fit to the data of Scharf *et al.* (1998), where tethered-cell CW bias was measured as a function of the concentration of the activated CheY mutant CheYD13KY106W. Inset, intracellular CheY concentrations as a function of IPTG induction of strain PS2001–pLC576. The number of CheY molecules/cell were determined using Western blots. CheY intracellular concentration was calculated assuming that 1000 molecules/cell correspond to 2.8 μM (Scharf *et al.*, 1998). The line is a smooth fit.

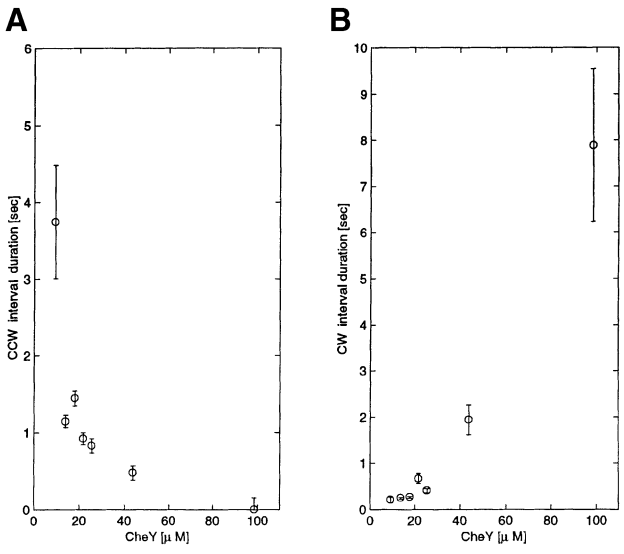

Fig. 2. Mean duration of CCW (**A**) and CW (**B**) intervals of tethered-cell rotation in PS2001–pLC576, as a function of intracellular CheY concentration.

Estimates of P-CheY levels in strains that contain wild-type levels of CheY

In order to estimate the fraction of CheY that is phosphorylated in wild-type cells, we employed the computerized tethering and swimming assays on strain RP437, the parental strain of all mutants used here, which

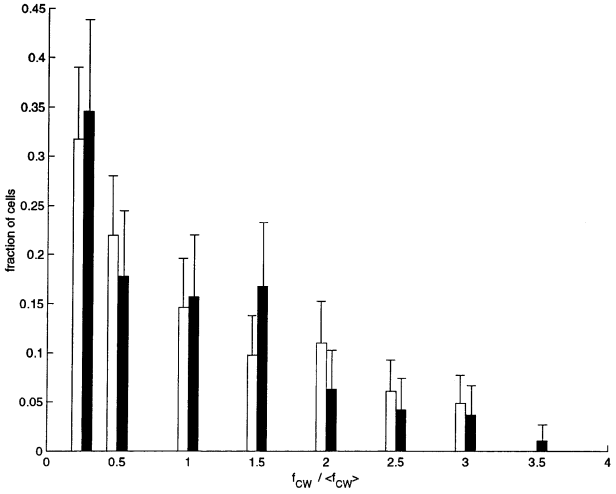

Fig. 3. Distribution of CW bias between different individual cells. Plotted is the fraction of time spent CW, f_{CW}, divided by the mean of f_{CW} over all cells with the same CheY induction level, $<f_{CW}>$. White bars, cumulative data from PS2001–pLC576 cells induced to a level of ~10, 14 and 20 μM CheY. Shaded bars, wild-type cells RP437–pHSG576. Error bars represent standard errors of the mean.

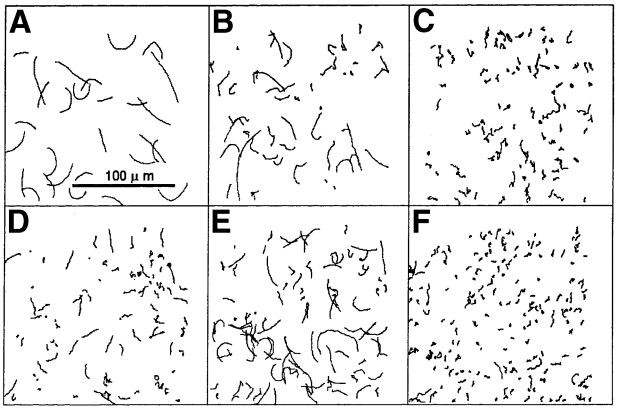

Fig. 4. Paths of swimming cells expressing varying amounts of P-CheY. Each path represents the trajectory of an individual bacterium over an average of ~2 s. (**A**) Strain deleted for *cheB*, *cheY* and *cheZ* (PS2001), the bar is 100 μm long, (**B**) PS2001–pLC576 expressing 10 ± 2 μM CheY, (**C**) PS2001–pLC576 expressing 60 ± 10 μM CheY, (**D**) PS2001–pLC576 expressing 100 ± 20 μM CheY, (**E**) RP437–pHSG576 (wild-type) and (**F**) RP1616–pHSG576 (Δ*cheZ*).

is wild-type for chemotaxis. We determined the total amount of CheY in RP437 under the present experimental conditions to be 17 500 ± 1000 molecules/cell (average ± SE of eight independent measurements), corresponding to a cytoplasmic concentration of ~49 ± 3 μM. This is close to the CheY levels in *Salmonella typhimurium* (15 000–20 000 CheY/cell; Stock *et al.*, 1985; Zhao *et al.*, 1996), but is ~3-fold higher than the value previously determined for the copy number in *E.coli* (Kuo and Koshland, 1987), perhaps due to the different growth conditions used in that study. In tethering assays, RP437 spent 0.22 ± 0.05 of the time turning CW (Figure 1). PS2001–pLC576 cells exhibited an equivalent behavior at a CheY concentration of ~13.5 ± 1 μM. Thus, in wild-type cells under these steady-state conditions ~30% of the intracellular pool of CheY is phosphorylated. The same conclusion was obtained from an analysis of swimming behavior. Wild-type cells exhibited a tumbling

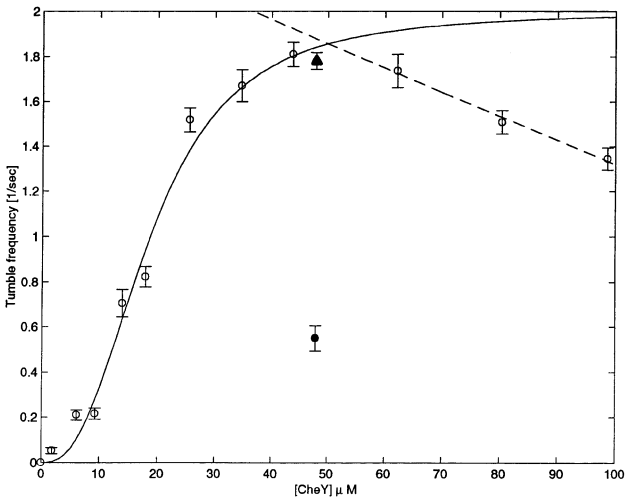

Fig. 5. Tumbling frequency as a function of CheY concentration. Open circles, PS2001–pLC576 induced with various amounts of IPTG; solid circle, wild-type (RP437–pHSG576); solid triangle, Δ*cheZ* (RP1616–pHSG576) cells. The tumbling frequency is the total number of tumbles detected by the computerized algorithm, divided by the total duration of all paths. The error bars represent standard errors of the mean. Solid line, fit to a Hill equation, with Hill coefficient of 2.5 and half maximal effect at 18.8 μM. Dashed line, guide to the eye.

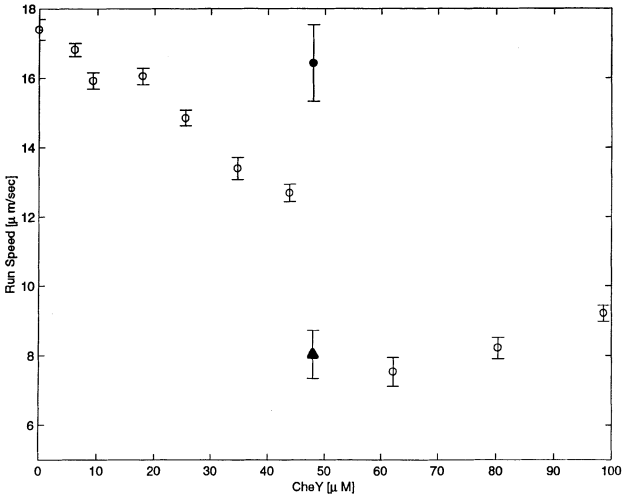

Fig. 6. Run speed as a function of CheY concentration in strain PS2001–pLC576 (open circles), wild-type (RP437–pHSG576) (solid circle) and Δ*cheZ* (RP1616–pHSG576) cells (solid triangle). Run speed is defined as the mean of the top 10% of the speeds along each bacterial trail, averaged over all trails. Shown are means ± SE of the mean.

frequency of 0.53 ± 0.05/s, and PS2001–pLC576 cells display the same tumbling frequency when the concentration of CheY is 13 ± 1 μM. Thus, the swimming assay also suggests that ~30% of the CheY is phosphorylated in RP437. The tumbling behavior and level of CheY expression in RP437 were not affected by the presence of the plasmid pHSG576, nor by growth in the presence of 50 μM IPTG (data not shown).

The swimming speed measured for wild-type cells (RP437) was 16.5 ± 1.0 μm/s (Figure 6). This is in good agreement with previous measurements where the cells were tracked near a glass slide (Amsler *et al.*, 1993; Khan *et al.*, 1993), though it is lower than some measurements of the run speed by three-dimensional tracking of cells

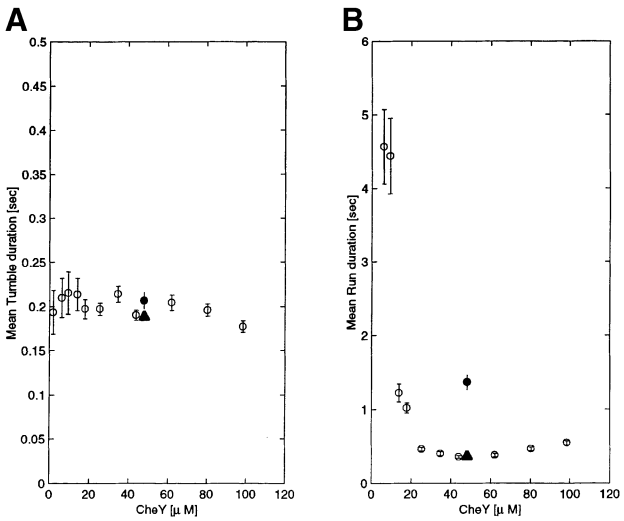

Fig. 7. Mean duration of tumbles (**A**) and runs (**B**), as a function of CheY concentration in PS2001–pLC576 in the wild-type strain (RP437–pHSG576) (solid circle) and Δ*cheZ* (RP1616–pHSG576) cells (solid triangle).

swimming far from any surface (Lowe *et al.*, 1987). In the present assay, the cells swim in a thin fluid layer at a distance of at most ~5 μm from a surface. Evidently, this has an effect on cell motion as compared with motion in a free solution (Ramia *et al.*, 1993; Frymier *et al.*, 1995; Vigeant and Ford, 1997). This of course should not affect the use of the present method as a read-out of the intracellular P-CheY levels.

The swimming behavior of RP1616–pHSG576 was also measured. This strain lacks the CheY phosphatase CheZ. Because of the CheZ defect, P-CheY levels are expected to be high in this strain (Table II), and in fact its tumbling frequency, 1.7 ± 0.1/s, is approximately equal to the maximal tumbling frequency of PS2001–pLC576 corresponding to wild-type levels of CheY (Figure 5). Thus, the observed RP1616 tumbling rate is consistent with the assumption that it contains a wild-type amount of CheY protein, essentially all in the phosphorylated state.

In vivo function of cheY mutants

The relation between P-CheY and tumbling frequency allowed us to compare quantitatively the *in vivo* activity of CheY mutants with that of wild-type P-CheY. Various amounts of the mutant proteins were expressed from inducible promoters, protein expression was quantified and swimming behavior was measured using the same procedure as for wild-type CheY. Two mutants were studied: CheYD13K, an activated mutant that causes tumbling in the absence of phosphorylation (Bourret *et al.*, 1993), and CheYD57A, a mutant that cannot be phosphorylated. The corresponding mutant genes were cloned into expression plasmids (Table I): *cheYD13K* was cloned into the low-copy vector pHSG576 under *lac* control, and *cheYD57A* into a complementary multicopy plasmid under an arabinose inducible promoter. The plasmids were transformed separately and together into the 'gutted' strain PS2002 that contains no Che genes (deleted from the beginning of *cheA* to the end of *cheZ*). Whereas the activated mutant CheYD13K caused tumbling (Figure 8), CheYD57A induced no tumbles even at

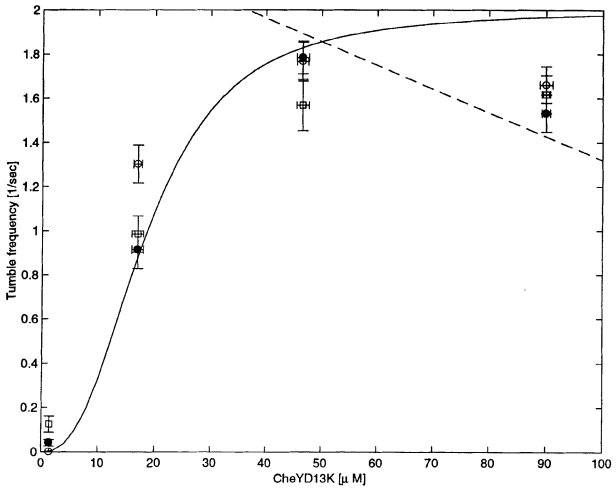

Fig. 8. Tumbling frequency as a function of mutant CheY proteins expressed in the gutted strain PS2002 which is deleted for *cheA–cheZ*. Open circles, PS2002–pMS164 induced with various amounts of IPTG expressing CheYD13K; solid circles, PS2002–pMS164–pMS168 induced with various amounts of IPTG expressing CheYD13K and CheYD57A, the latter induced with 0 μM arabinose; open squares, PS2002–pMS164–pMS168 induced with 100 μM arabinose and varying amounts of IPTG (CheYD13K coexpressed with CheYD57A, the latter at an intracellular concentration of 260 ± 40 μM). The solid and dashed lines represent the tumbling frequency induced by wild-type CheY in strain PS2001 (from Figure 5).

intracellular concentrations >200 μM (data not shown). Moreover, swimming behavior as a function of CheYD13K concentration was not affected by simultaneous expression of >200 μM CheYD57A (Figure 8). Thus, unphosphorylated CheY does not appear to compete with active CheY for binding to the motor, and does not appear to cause either tumbles or runs. This result is consistent with the *in vitro* studies of CheY binding to FliM where it has been shown that CheY binding to the motor switch protein is substantially enhanced by phosphorylation (Welch *et al*., 1993, 1994).

The activated mutant, CheYD13K, had approximately the same quantitative effect *in vivo* as P-CheY (Figure 8). This finding was unexpected; previous *in vitro* studies have indicated that CheYD13K binds FliM only marginally more avidly than unphosphorylated CheY (Welch *et al.*, 1994), and it has also been shown that the crystal structure of CheYD13K is similar to that of unphosphorylated CheY (Jiang *et al*., 1997). Our results therefore raise the possibility that CheYD13K behaves somewhat differently *in vivo* and *in vitro*. The measurement of CheYD13K activity complements a recent study relating tethered motor rotation to the level of the activated CheY mutant CheYD13KY106W (Scharf *et al.*, 1998). In that study, a dependence of CW bias on the activated CheY mutant level was established, which is quantitatively similar to the relation we observe between CW bias and wild-type P-CheY (Figure 1). The similarity in behavior is consistent with an approximately equivalent activity of CheYD13-KY106W and P-CheY.

Finally, it is worth noting that wild-type CheY expressed in the gutted strain, PS2002, did not induce tumbling even at levels of ~100 μM (data not shown). This indicates that sources of CheY phosphorylation other than the chemotaxis network are negligible *in vivo* under the conditions used.

Discussion

Molecular mechanism of signal transduction

The present study establishes a quantitative relationship between measurable parameters of cell behavior (motor rotation, tumbling frequency, speed) and the output of the chemotaxis signal transduction network (P-CheY). This enables determination of the P-CheY levels in wild-type cells (~30% under steady-state conditions) and evaluation of the activity of CheY mutants. Most importantly, this relationship forms a basis for the quantitative evaluation of molecular models of the chemotaxis network. For instance, we find that swimming behavior is relatively insensitive to changes in the level of P-CheY (apparent Hill coefficient ~2.5). Similarly, tethered cell CW bias has an apparent Hill coefficient of ~3.5. It has been established, however, that *E.coli* is highly sensitive to small changes in attractant concentrations (Berg and Brown, 1972; Segall *et al.*, 1986; Khan *et al.*, 1993). Attempts to use the known biochemistry to model chemotaxis have accounted for this high sensitivity by assuming a highly cooperative interaction between P-CheY and the motor [apparent Hill coefficients ranging from 8 to 11 (Ninfa *et al.*, 1991; Spiro *et al.*, 1997)]. From this discrepancy, we can conclude that the high sensitivity of the chemotaxis system must derive from some additional, hitherto undefined, biochemical interactions in the receptor-mediated control of CheY phosphorylation.

Relationship between tethered motor rotation and swimming behavior

We have directly compared the behavior of tethered and swimming cells under the same conditions. It is well-established that increased CW motor rotation generally corresponds to a higher tumble frequency. Quantitative comparisons, however, reveal clear differences (Ishihara *et al*., 1983). In tethered cells CW intervals become longer and CCW intervals become shorter with increasing P-CheY concentration (Figure 2). If there were a direct correlation between CW rotation and tumbling, one would expect tumbling intervals to become longer as CW rotation increases, and this was not observed. The average duration of tumbles was found to be 0.20 ± 0.05 s, independent of CheY concentration (Figure 7). This extends the findings of Berg and Brown (1972), who reported an equal mean tumble duration (~0.14 s) in several strains, including a wild-type strain and a tumbly mutant. In contrast, the mean duration of runs decreased dramatically with P-CheY concentration (Figure 7), from continually running in the absence of P-CheY down to 0.3 s runs at the maximally tumbly P-CheY concentration (~50 μM). Thus, it appears that during chemotaxis the bacteria mainly modulate the duration of their runs, keeping their tumbles brief.

It seems likely that the observed lack of correlation between the duration of CW intervals and tumbles is primarily due to the details of bundle reformation after a tumble. In returning to a run state, the flagella must restore contact with one another and re-assemble into a bundle (Khan *et al.*, 1978; Macnab, 1996). This may occur gradually (Berg and Brown, 1972) where first a partial bundle is formed that begins to propel the cell and the ensuing fluid velocity sweeps back the other flagella to

re-constitute a full bundle. A crude estimate of the typical time for such hydrodynamic interactions is the bacterium length (a few micrometers) divided by its velocity (10–20 μm/s), yielding a tumble duration of the order of tenths of seconds. One may view the flagella interactions as an additional level of information processing in the chemotaxis response. The result of this processing is that whereas individual motors display prolonged CW intervals, swimming cells keep their tumble duration short and independent of P-CheY. This behavior of swimming cells is close to the expected optimal behavior. Since it is only during runs that the bacteria sample their environment and reach favorable regions, each tumble should be kept as brief as is necessary to randomize the heading of the subsequent run.

An additional difference between tethered motors and free-swimming cells is observed at very high P-CheY levels. Whereas CW rotation increases monotonically (Figure 1), swimming cells become less tumbly at P-CheY levels higher than ~50 μM (Figures 4 and 5). This is probably caused by the runs associated with CW rotating bundles that have previously been documented in flagella switch mutants that lock the motor in an extreme CW state (Khan *et al.*, 1978; Wolfe and Berg, 1989). The average run speed drops abruptly at high P-CheY levels to ~50% of the wild-type run speed (Figure 6), in agreement with the observation that speed generated by CW bundles is about half the speed generated by CCW bundles (Khan *et al.*, 1978). It should be noted that CW runs only predominate at P-CheY levels that exceed the total CheY content of wild-type cells. At all levels of P-CheY that could possibly be attained in wild-type cells (i.e. 0 to ~50 μM), the tumbling frequency increases with increasing P-CheY. It is only at P-CheY levels exceeding the maximal physiological level that the tumbling frequency begins to decrease with increasing P-CheY. This latter behavior can be detrimental since it leads to reverse chemotaxis where cells move towards repellants and away from attractants (Khan *et al.*, 1978). Strikingly, the cell appears to have tuned the signal transduction pathway (kinase activity and CheY concentration) to give the highest possible maximal tumbling response that does not carry over to the reverse chemotaxis regime.

Molecular mechanism of response regulation

There appear to be ~30 potential binding sites for P-CheY at each motor (Macnab, 1995; Zhao *et al.*, 1996). From this one might expect a high degree of cooperativity in P-CheY-induced switching. The motor CW rotation fraction appears, however, to have a low order dependence on P-CheY (apparent Hill coefficient, 3.5 ± 1.0; Hill coefficient of ~4.2 in Scharf *et al.*, 1998). The tumbling frequency of swimming cells exhibits an even lower order dependence on P-CheY (apparent Hill coefficient, 2.5 ± 1.0). In order to reconcile the high number of binding sites with the observed lack of strong cooperativity, we propose an allosteric model of P-CheY-induced motor switching. The model extends the model of Macnab (1995) and related analyses by Block *et al.* (1983) and Turner *et al.* (1996).

The model is based on the classical model of allosteric enzymes (Monod *et al.*, 1965). The entire motor, a large multi-protein ensemble, is considered as an allosteric switch. The motor is assumed to display equilibrium

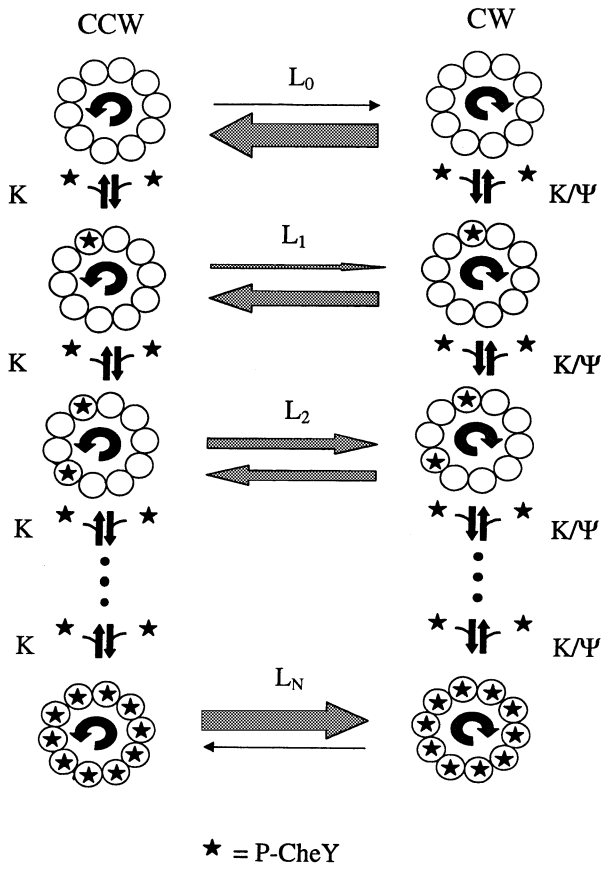

Fig. 9. Allosteric model for the motor switch. The motor is assumed to be in one of two states, CCW or CW. It displays spontaneous stochastic transitions between the states, with a (large) equilibrium constant L_0. The motor is assumed to have N independent, identical binding sites (represented here by open circles) for P-CheY (stars). Both of the rotation states can display multiple P-CheY occupancy states, with between 0 and N sites bound by P-CheY proteins. The probability of P-CheY binding is not the same for the two states. The equilibrium dissociation constants for P-CheY binding are K for binding to the CCW state and K/Ψ for binding to the CW state (vertical arrows). Transitions between CW and CCW states with m binding sites occupied by P-CheY occur with equilibrium constants L_m (horizontal arrows). In the model, P-CheY binds preferentially to the CW state ($\Psi > 1$), and thus increasing cytoplasmic concentrations of P-CheY shift the equilibrium towards a higher fraction of time spent in the CW state.

stochastic concerted transitions between two discreet conformational states, CCW and CW (Figure 9). P-CheY is assumed to bind with greater affinity to the CW state, and therefore high P-CheY levels shift the equilibrium towards CW rotation. The fraction of time the motor spends turning CW is given by the expression:

$$f_{CW} = [1 + \Psi\,(\text{P-CheY})/K\,]^N/[(1 + \Psi\,[\text{P-CheY}]/K\,)^N + L_0\,(1 + [\text{P-CheY}]/K\,)^N]$$

where N is the number of P-CheY binding sites in a motor switch complex, L_0 is the equilibrium constant for spontaneous concerted transitions between the CCW and CW states (Turner *et al.*, 1996), and K and K/Ψ are the equilibrium dissociation constants of P-CheY to the CCW and CW states, respectively. The model can be fit to the experimental data (Figure 1), using reasonable values for the parameters. For example, assuming $N = 30$ binding sites per motor, and $L_0 = 10^7$ (Turner

et al., 1996), the best fit value of the P-CheY equilibrium constant K is 7.6 ± 2 μM, and Ψ, which corresponds to the ratio in P-CheY binding affinity to the CW and CCW states, is 2.0 ± 0.2. One important prediction of the model is that to obtain the observed weak cooperativity with a large number of P-CheY binding sites implies that there can only be a relatively small difference in P-CheY affinity for the CW and CCW states (~2-fold, Ψ ~2). This is similar to the prediction of a related model by Scharf *et al*. (1998), in which the free energy of the CCW state increases and that of the CW state decreases by a small amount with each P-CheY bound.

Fitting data to a model does not, of course, constitute a validation of the model's assumptions. We hope, however, that this model can serve as a simple basis for comparison for future experiments that could shed light on the switch mechanism. For example, the model supplies a way of understanding the effects of mutations of Tyr106 in CheY (Zhu *et al*., 1996). Cells with these mutations are deficient in chemotaxis despite the fact that these CheY variants can be phosphorylated and show a phosphorylation-dependent binding to FliM that is comparable with the wild-type CheY protein. In view of the present model, these mutations might affect the preferential binding of the mutant CheY to the CW state (i.e. these mutations could affect Ψ). We would predict that a mutation that caused P-CheY to bind more strongly to the CCW state would be a dominant suppressor of tumbling caused by wild-type CheY. The idea that differential binding to the two motor states is required for switching could explain the observation that the binding of P-CheY to the motor and the generation of tumbles appear to be mutationally separable events (Bourret *et al.*, 1990; Welch *et al.*, 1994; Ganguli *et al*., 1995).

Conclusions

Previous work has elucidated many of the quantitative interactions of chemotaxis network components, as well as many aspects of behavioral physiology. The present work connects these two modes of description by establishing the precise dependence of measurable cell behavior on the response regulator output of the signal transduction network (P-CheY). This allows the direct experimental assessment of theoretical analyses, and allows the identification of gaps in our understanding of the biochemistry of chemotaxis signal transduction. For instance, we can now say that the molecular mechanisms responsible for the high sensitivity of the chemotaxis system to small changes in attractant stimuli are yet to be elucidated.

Materials and methods

Bacterial strains and plasmids

All strains were derived from an *E.coli* K-12 derivative, RP437, which is wild-type for chemotaxis. RP437 and RP1616 (Δ*cheZ*) were obtained from Dr J.S.Parkinson. The strains PS2001 (Δ*cheBcheYcheZ*) and PS2002 (Δ*cheA–cheZ*) were constructed from RP437 by the overlap extension method (Ho *et al.*, 1989), using the gene replacement vector pK03 (gift of Dr G.Church). Briefly, genomic DNA from RP437 was used as template to amplify two DNA fragments that flank the chemotaxis genes to be deleted by the polymerase chain reaction (PCR). For PS2001 the primers cheRF1 (5′-CAGGGATCCGAGCGCCTGGCGCTTTCC), and cheRR1 (5′-CTGGTATCGAATTCGTTAATCCTTACTTAGCGC), were used to amplify a 814 bp *cheR* fragment that includes the *cheR* stop codon; a 1132 bp fragment from the end of *cheZ* to *flhB* was amplified using the primers cheZF1 (5′-GGATTAACGAATTCGATACCAGCAAAGCCGGTG), and flhBR1 (5′-CTCGCTGCATCTGACGGATCCGCC). For construction of PS2002, a 634 bp fragment from *motB* that includes the stop codon of *motB*, was amplified using the primers motBF1 (5′-CGTGGATCCGCAGCCGAACATCGAAGAGCTG), and motBR1 (5′-GTATCGACCGAATTCTGTCACCTCGGTTCGGCTG); a 757 bp fragment from the end of *cheZ* to the middle of *flhB* was obtained using the primers cheZF2 (5′-GTGACAGAATTCGGTCGATACCAGCAAAGCCGG) and flhBR2 (5′-GAAGGATCCCCGTCACGCTGCCAACCAGG). These fragments were purified and cloned into pTZ19R (Pharmacia) which has been previously modified to eliminate the recognition sequence of *Eco*RI endonuclease. A resistance marker (Kan^R) was cloned into an *Eco*RI site present in the linker region used to generate the deleted fragment. The complete insert was excised using *Bam*HI, and ligated into the *Bam*HI site in pKO3. The resulting construct was used to transform RP437 selecting for Kan resistance. At its non-permissive temperature (42°C), pKO3 cannot replicate and genomic integrants are selected. At the permissive temperature (30°C) recombinants are selected that have lost the plasmid. The sequence of all PCR-generated fragments was determined to ensure no errors were introduced in the sequence during the amplification reaction. Confirmation of the deletions was obtained by PCR.

CheY was expressed under control of *lacOP* using the low copy plasmid pLC576 (Cm^R). This plasmid was engineered by cloning a DNA fragment encoding *E.coli* CheY, generated by PCR, into the polylinker region of pUC-lac1 (Surette and Stock, 1996). A fragment carrying the *lac-I*^{q} gene as well as *lacOP-cheY* from the resulting construct was cloned into the polylinker region of the low-copy-number plasmid pHSG576 (Takeshita *et al.*, 1987). The *cheY* gene in this plasmid was sequenced to ensure no errors were introduced during amplification. The *cheYD13K* and D57A mutations were generated by site-directed mutagenesis using standard protocols and subsequently, the *cheYD13K* gene was cloned into pLC576 (replacing the wild-type *cheY* gene) to generate pMS164 and the *cheYD57A* gene was cloned into pBAD18 (Guzman *et al.*, 1995) to generate pMS168. We note that a different unphosphorylatable mutant, CheYD57N, was found to cause some tumbles when expressed at high levels (data not shown).

Isolation of plasmid DNA was carried out using Qiaprep spin columns (Qiagen). PCR was performed using Ultima enzyme (Perkin Elmer Cetus) or Pfu polymerase (Stratagene) according to the supplier's instructions. DNA sequencing reactions were done by the dideoxy method using modified T7 DNA polymerase Sequenase (UA Biochemical) or were carried out by the Oligonucleotide Sequencing/Synthesis Facility, Department of Molecular Biology, Princeton University, NJ.

Behavioral assays

Strains were grown overnight in Tryptone broth (1.3% Bacto tryptone and 0.7% NaCl) at 30°C and diluted 1:50 into Tryptone broth supplemented with selective antibiotics as appropriate. After 1.5 h of growth, the cultures were induced with IPTG and/or arabinose. The cells were harvested at mid-log phase (OD_{600} = 0.50 ± 0.03, corresponding to 5.3×10^8 ± 0.3×10^8 cells/ml). A sample from each culture was pelleted and frozen at –20°C for quantitation of CheY (see below). Cells from 1 ml of culture were harvested by centrifugation at 800 *g* for 5 min at room temperature and gently resuspended into 1 ml motility medium [7.6 mM $(NH_4)_2$ SO_4, 2 mM $MgSO_4$, 20 μM $FeSO_4$, 0.1 mM EDTA, 60 mM potassium phosphate pH 6.8], centrifuged at 800 *g* for 5 min at room temperature and gently resuspended in a final volume of 0.5 ml motility medium.

For swimming behavior, 0.5 μl of this suspension was placed on a glass slide (Gold Seal) in the center of a circle inscribed by a grease pencil, and covered by a No. 2 coverslip (Corning). This created a fluid layer of ~10 μm thickness, as estimated from the area of the fluid film. The cells were thus confined to motion in two dimensions, and could not move out of the focal plane of the microscope. After 5 min, the samples were observed with a Zeiss Dialux dark field microscope mounted with a video camera and swimming behavior was recorded for several minutes on a JVC S-VHS video recorder. The field of view spanned 180 μm; 30 s segments of the video were analyzed by computerized image analysis as described below.

For tether analysis, 400 μl of the cell suspension was passed through a 28 gauge needle 40–60 times to shear the flagella. The cells were harvested and washed by centrifugation as described above. A 20 μl drop of the suspension was placed under a coverslip mounted on a glass slide and sealed with paraffin. The coverslip (No. 1.5, Corning) was pretreated with anti-flagellin polyclonal antibodies for 20 min and then

washed with motility media. The cells were allowed to attach to the coverslip for 15–30 min. The tethered cells were observed with a Zeiss Dialux dark-field microscope mounted with a video camera and behavior was recorded for several minutes for each of several fields of view on a JVC S-VHS video recorder. Segments of the video were analyzed as described below.

Preliminary experiments showed that cells washed into another commonly used chemotaxis buffer (67 mM NaCl, 0.1 mM EDTA, 10 mM potassium phosphate pH 7.0; Scharf *et al.*, 1998) displayed the same tumbling frequency as cells washed into the present motility medium. In general, however, when comparing results from chemotaxis assays performed under different conditions, it is worth noting that there are factors that can affect motor behavior independently of CheY phosphorylation (Khan and Macnab, 1980; Montrone *et al.*, 1996; Turner *et al.*, 1996; Barak *et al.*, 1998).

Computerized image analysis of swimming cells

Video images at 30 frames/s, at a resolution of 640×480 pixels, were loaded into computer memory using a Silicon Graphics Indy workstation with a Cosmo real-time video compression/decompression board. Images were digitally thresholded, and clusters of pixels above the threshold intensity were detected and their center of mass was recorded, each representing one bacterium. Bacteria in successive frames were grouped into 'trails', where each trail represented the trajectory of a bacterium. Trails were terminated when a bacterium left the screen or overlapped with another cell. This software was implemented in C++. Tumbles were detected by processing trail data with an algorithm implemented in Matlab (Mathworks). The algorithm extends the computerized tumble-detector of Amsler (1996), allowing accurate quantitation of tumbles in a wide range of phenotypes from continually running to very tumbly. The tumble-detection software accepted a file containing the list of bacteria center of mass positions for each trail. Trails shorter than 1 s were discarded. In order to reduce the noise in the data, and yet to preserve sharp transitions in the bacteria trajectory, the trails were filtered using a modified median filter. In this filter, a window of five time points is considered, the five are sorted and the filtered value is given by the average of the central three sorted points. The speed of each bacterium as a function of time, V, is calculated, as is the rate of change of direction (RCD; angular velocity) of the trajectory: $RCD = |A_xV_y - V_xA_y|/V^2$, where V_x and V_y are the x and y components of the velocity, and A_x and A_y are the x and y components of the bacteria acceleration. RCD (Khan *et al*., 1992) has units of rad/s. RCD was employed for characterizing the chemotactic response of wild-type and mutant bacteria in recent studies (Khan *et al.*, 1993, 1995).

Plotting the bacterial speed as a function of time reveals a signal which can be roughly characterized by two states: periods of high speed (>10 μm/s) are punctuated by short spans of low speed (<5 μm/s). The angular velocity, RCD, has the inverse behavior: it tends to be low (of the order 0.1 rad/s) when the bacterium is fast, and displays pronounced peaks (of the order 1–10 rad/s), which represent rapid reorientation of the bacterium's heading, correlated with low V intervals. In the tumble detection algorithm, the high V, low RCD regions are identified as runs, and the low V, high RCD intervals as tumbles. The following criterion is used. The run speed, V_R, for each trail is defined as the average of the top 10% of the speed in the trail. A tumble is detected at times when both $V < 0.5 \times V_R$ and RCD >3 rad/s. These threshold values were selected so that the tumble detector agrees best with manually collected data. Comparing the tumble detector with a set of 200 manually analyzed trails of wild-type RP437 bacteria, each on average 5 s long, the algorithm correctly identifies 96% of the tumbles, and has an additional 5% 'false-positive' detections where no tumble was observed by eye. In addition, a manual estimate of the tumbling rate was performed in parallel to the automatic analysis, for PS2001–pLC576 cells in which P-CheY was induced to yield cells which span the entire range of phenotypes from continually running to highly tumbly. In each recording, the tumble frequency was manually measured by counting the number of tumbles that occur in 20 different cells, each followed for a 5 s interval. The discrepancy between the manual and the computerized mean tumble frequency was <20% in all cases. The sensitivity of the results to the tumble detection threshold values was checked on the 200 wild-type trail data set. The value of the speed threshold could be changed between $0.4 \times V_R$ and $0.6 \times V_R$ yielding a <10% change in the tumble frequency and a 15% change in the mean tumble duration. The RCD threshold could be varied in the range 1.5–6 rad/s, with a <10% change in tumble frequency and a <30% change in mean tumble duration. The detection of a tumble is less sensitive to the precise definition of a tumble than the measurement of the tumble duration. Video movies of some of the cells were analyzed at double the temporal resolution, 60 frames/s, and the same mean tumble duration was obtained.

Cells adhering to the coverslip or slide were automatically discarded by the software. The criterion for rejection was that the maximal displacement of the bacterium during a trail is <5 μm. In addition, some small percentage of the population swam in an abnormal jittery fashion, presumably due to some defect in the cell or its flagella (Dowd and Matsumura, 1997). These cells could contribute significant fluctuations to the tumble frequency if not discarded. Therefore, the trails were sorted by tumble frequency, and the top and bottom 10% were discarded. This criterion eliminated outlier cells and improves the reproducibility of the tumble detector.

Computerized image analysis of tethered cells

Video movies of the tethered cells were recorded on a VCR. The video movies were analyzed by computerized image-processing, at a rate of 60 frames/s, using the same software as for the swimming cells. The trails were not subjected to filtering with the modified median filter, in order to increase the temporal resolution of the system, and to detect rapidly turning cells. The RCD of all cells in the field of view was calculated as described above. Rotating cells were selected according to the following criterion: the position of the peak in the distribution of angular velocities of the cell had to be greater in absolute value than 2 Hz (RCD >4 π rad/s). This effectively rejects stuck and diffusing cells, since their angular velocity is strongly peaked at zero. A field of view typically contained 20–100 motionless bacteria, and one to four rotating tethered bacteria. One hundred-second movies of each field of view were analyzed. Some rotating cells intermittently paused or got stuck (Eisenbach *et al.*, 1990). These intervals were discarded from the analysis. The statistics of the tethered-cell motion were analyzed using specially written Matlab software. CCW intervals corresponded to a negative RCD, and CW intervals to a positive RCD. We estimate that the shortest interval detectable by this system is ~50 ms (three frames).

CheY quantitation

We determined the total amount of CheY in RP437–pHSG576 under the present experimental conditions to be 17 500 ± 1000 molecules/cell (average ± SE of eight independent measurements) as follows. Cell density was determined by viable cell count on nutrient agar. A 1.0 ml sample from each culture was pelleted, resuspended in gel loading buffer, boiled for 10 min at 100°C, and subjected to 15% SDS–PAGE. Standards were prepared by adding known amounts of purified CheY to the same number of cells of the gutted strain, PS2002–pHSG576. Each gel contained two sets of three or four standards, and duplicate sample lanes. Proteins were transferred to nitrocellulose membranes (0.2 μm; Millipore) and probed with affinity-purified rabbit anti-CheY antibodies. The immunoblots were assayed using the Western Star chemiluminescence kit (Tropix) and exposed to X-Omat film (Kodak). Band intensities were quantitated by scanning the developed film and analyzing the images with NIH-Image software. Levels of CheY expression in all other strains were determined relative to those in the wild-type, RP437–pHSG576. Samples from these strains that had been stored frozen at –20°C were resuspended in lysis buffer (0.9% NaCl, 0.75% SDS) and boiled for 10 min at 100°C. Total protein was determined using the BCA assay (Pierce) with BSA standards prepared in lysis buffer. Aliquots of 8 μg of protein from each sample were subjected to 15% SDS–PAGE. Samples with levels of CheY greater than wild-type were first diluted with extracts prepared from the gutted strain, PS2002–pHSG576. Standards which bracket the samples, each containing 8 μg of protein, were run on the same gels. These were prepared by mixing various amounts of wild-type RP437–pHSG576 with gutted cell extract. Each gel contained two sets of three or four standards, and duplicate sample lanes. Proteins were transferred to nitrocellulose membrane and estimates of CheY levels were determined as described above. The amount of CheY per cell was then calculated using the above measurement for the wild-type CheY level. Concentrations of mutant CheY proteins were measured using the same procedure, against RP437 standards mixed with appropriate amounts of PS2002–pHSG576. In all immunoblot quantitations, the intensity of the standard bands was linear with the CheY content of the standards, and the standards bracketed the sample intensities. The CheY levels presented are the averages of several independent determinations. CheY concentrations were calculated assuming that 1000 molecules/cell correspond to a concentration of 2.8 μM (Scharf *et al.*, 1998). Total protein per cell was not affected by CheY expression, as determined using the BSA assay (Pierce) against BSA standards prepared in lysis buffer.

Electron microscopy

The number of flagella per cell was determined for RP437 and IPTG-induced PS2001–pLC576 cells grown as for the behavioral assays. Cells were harvested at 800 *g* and resuspended gently in motility medium. The cells were allowed to attach to a Formvar-coated grid for 2 min, and then stained with 1% uranyl acetate. Flagella were counted as the number of filaments that emerge from the cell body; at least 25 cells from each growth condition were registered.

Modeling the motor switch

Here we give further details of the allosteric model of the motor switch described in the Discussion and Figure 9. Let $[CCW_m]$ denote the probability that the motor is in the CCW state with m P-CheY proteins bound, and $[CW_m]$ denote the probability that the motor is in the CW state with m P-CheY bound, with m in the range 0–N. At equilibrium, the ratio between these probabilities is given by $[CCW_m]/[CW_m] = L_m$. P-CheY binding is described by equilibrium dissociation constants, with $[CCW_{m-1}]\times[\text{P-CheY}]/[CCW_m] = K$, and $[CW_{m-1}]\times[\text{P-CheY}]/[CW_m] = K/\Psi$, where [P-CheY] is the cytoplasmic concentration of P-CheY. Detailed balance considerations, relating the equilibrium constants along closed loops in the reaction diagram (Figure 9), show that $L_m = L_0/\Psi^m$ (Turner *et al*., 1996). Thus the model is determined by four parameters: N, the number of binding sites; K, the binding constant of P-CheY to the CCW state; Ψ, the ratio between binding to the CW and CCW states; and L_0, the 'allosteric' constant, which corresponds to spontaneous switches of the motor in the absence of CheY. Taking into account the combinatorial factor corresponding to the number of patterns of site occupancy that apply to each state, one finds that $[CW_m] = [CW_0]y^m\Psi^m$ N!/m! (N – m)!, and $[CCW_m] = L_0[CW_0]y^m$ N!/m! (N – m)!, where $y = [\text{P-CheY}]/K$. The fraction of time the motor spends turning clockwise is given by equation 1 (see Discussion). This equation is identical to the equation describing classical allosteric enzymes (Monod *et al*., 1965), despite some minor differences in the model formulation. The CCW state corresponds to the 'R' state and the CW state to the 'T' state in the original allosteric model. The model could be used to fit the experimental data for f_{CW} (Figure 1). Satisfactory fits can be obtained for a range of the values of the parameters L_0 and N. In particular, any number of binding sites greater than five and allosteric constants larger than $\sim 10^3$ allow fits of similar quality to that shown in Figure 1. In Figure 1, the values N = 30 and $L_0 = 10^7$ were chosen based on previous estimates (Macnab, 1995; Turner *et al*., 1996). Once N and L_0 are chosen, the best-fit value of the other two parameters, *K* and Ψ, are found to fall in a more restricted range. For N in the range 5–100 and L_0 in the range 10^3–10^9, the range of *K* and Ψ variation is K = 2–12 μM and Ψ = 1.1–2.5. When varying the measured tethered data within its error bars, the standard deviation of the best-fit parameters is 10–20%. The best-fit value of Ψ becomes closer to 1 with increasing number of binding sites. The model curve in Figure 1 that corresponds to the data of Scharf *et al.* (1998) is a best fit, using N = 30 and $L_0 = 10^7$, to eqn 3 of Scharf *et al.* (1998), with the parameters ΔG_0 = 14.4 kT, Mr = 23.1 kT, and K_D = 9.1 μM as given in that paper. Best fits were carried out using the *fmins* function of Matlab 4.2 (Mathworks), using default settings.

Acknowledgements

We thank J.S.Parkinson for bacterial strains, and R.Macnab, L.Turner, H.C.Berg, S.Block, J.P.Dowd, M.Elowitz, P.Cluzel, C.Guet and N.Barkai for helpful discussions. U.A. was supported by Rothchild and Markee fellowships. L.C. was supported by a Pew fellowship. This work was supported by PHS grant AI20980 (to J.B.S.).

References

Amsler,C.D. (1996) Use of computer-assisted motion analysis for quantitative measurements of swimming behavior in peritrichously flagellated bacteria. *Anal. Biochem*., **235**, 20–25.

Amsler,C.D., Cho,M. and Matsumura,P. (1993) Multiple factors underlying the maximal motility of *Escherichia coli* as cultures enter post-exponential growth. *J. Bacteriol.*, **175**, 6238–6244.

Barak,R., Abouhamad,W.N. and Eisenbach,M. (1998) Both acetate kinase and acetyl coenzyme A synthetase are involved in acetate-stimulated change in the direction of flagellar rotation in *Escherichia coli*. *J. Bacteriol*., **180**, 985–988.

Barkai,N. and Leibler,S. (1997) Robustness in simple biochemical networks. *Nature*, **387**, 913–917.

Berg,H.C. and Brown,D.A. (1972) Chemotaxis in *Escherichia coli* analyzed by three-dimensional tracking. *Nature*, **239**, 500–503.

Berg,H.C. and Tedesco,P. (1975) Transient response to chemotaxis stimuli in *Escherichia coli*. *Proc. Natl Acad. Sci. USA*, **72**, 3235–3239.

Borkovich,K.A., Alex,L.A. and Simon,M.I. (1992) Attenuation of sensory receptor signaling by covalent modification. *Proc. Natl Acad. Sci. USA*, **89**, 6756–6760.

Bourret,R.B., Drake,S.K., Chervitz,S.A., Simon,M.I. and Falke,J.J. (1993) Activation of the phosphosignaling protein CheY. 2. Analysis of activated mutants by F^{19} NMR and protein engineering. *J. Biol. Chem*., **268**, 13089–13096.

Block,S.M., Segall,J.E. and Berg,H.C. (1983) Adaptation kinetics in bacterial chemotaxis. *J. Bacteriol*., **154**, 312–323.

Bray,D. and Bourret,R.B. (1995) Computer analysis of the binding reactions leading to a transmembrane receptor-linked multiprotein complex involved in bacterial chemotaxis. *Mol. Biol. Cell*, **6**, 1367–1380.

Bray,D., Bourret,R.B. and Simon,M.I. (1993) Computer simulation of the phosphorylation cascade controlling bacterial chemotaxis. *Mol. Biol. Cell*, **4**, 469–482.

Dowd,J.P. and Matsumura,P. (1997) The use of flash photolysis for a high-resolution temporal and spatial analysis of bacterial chemotactic behaviour: CheZ is not always necessary for chemotaxis. *Mol. Microbiol*., **25**,295–302.

Eisenbach,M. (1996) Control of bacterial chemotaxis. *Mol. Microbiol*., **20**, 903–910.

Eisenbach,M., Wolf,A., Welch,M., Caplan,S.R., Lapidus,R.I., Macnab,R.M., Aloni,H. and Asher,O. (1990) Pausing, switching and speed fluctuation of the bacterial flagellar motor and their relation to motility and chemotaxis. *J. Mol. Biol*., **211**, 551–563.

Falke,J.J., Bass,R.B., Butler,S.L., Chervitz,S.A. and Danielson,M.A. (1997) The two-component signaling pathway of bacterial chemotaxis: A molecular view of signal transduction by receptors, kinases and adaptation enzymes. *Annu. Rev. Cell Dev. Biol*., **13**, 457–512.

Frymier,P.D., Ford,R.M., Berg,H.C. and Cummings,P.T. (1995) Three-dimensional tracking of motile bacteria near a solid planar surface. *Proc. Natl Acad. Sci. USA*, **92**, 6195–6199.

Ganguli,S., Wang,H., Matsumura,P. and Volz,K. (1995) Uncoupling phosphorylation and activation in bacterial chemotaxis: the 2.1 Å structure of threonine to isoleucine mutant at position 87 of CheY. *J. Biol. Chem*., **270**, 17386–173933.

Guzman,L.M., Belin,D., Carson,M.J. and Beckwith,J. (1995) Tight regulation, modulation and high-level expression by vectors containing the arabinose PBAD promoter. *J. Bacteriol*., **177**, 4121–4130.

Hauri,D.C. and Ross,J. (1995) A model of excitation and adaptation in bacterial chemotaxis. *Biophys. J*., **68**, 708–722.

Hess,J.F., Oosawa,K., Kaplan,N. and Simon,M.I. (1988) Phosphorylation of three proteins in the signaling pathway of bacterial chemotaxis. *Cell*, **53**, 79–87.

Ho,S.N., Hunt,H.D., Horton,R.M., Pullen,J.K. and Pease,L.R. (1989) Site-directed mutagenesis by overlap extension using the polymerase chain reaction. *Gene*, **77**, 51–59.

Ishihara,A., Segall,J.S., Block,S.M. and Berg,H.C. (1983) Coordination of flagella on filamentous cells of *Escherichia coli*. *J. Bacteriol*., **155**, 228–237.

Jiang,M., Bourret,R.B., Simon,M.I. and Volz,K. (1997) Uncoupled phosphorylation and activation in bacterial chemotaxis. The 2.3 Å structure of an aspartate to lysine mutant at position 13 of CheY. *J. Biol. Chem*., **272**, 11850–11855.

Khan,S. and Macnab,R.M. (1980) The steady-state counterclockwise/clockwise ratio of bacterial flagellar motors is regulated by protonmotive force. *J. Mol. Biol*., **138**, 563–597.

Khan,S., Macnab,R.M., DeFranco,A.L. and Koshland,D.E.,Jr (1978) Inversion of a behavioral response in bacterial chemotaxis: explanation at a molecular level. *Proc. Natl Acad. Sci. USA*, **75**, 4150–4154.

Khan,S., Amoyaw,K., Spudich,J.L., Reid,G.P. and Trentham,D.R. (1992) Bacterial chemoreceptor signaling probed by flash photorelease of a caged serine. *Biophys. J*., **62**, 67–68.

Khan,S., Castellano,F., Spudich,J.L., McCray,J.A., Goody,R.S., Reid,G.P. and Trentham,D.R. (1993) Excitatory signaling in bacteria probed by caged chemoeffectors. *Biophys. J*., **65**, 2368–2382.

Khan,S., Spudich,J.L., McCray,J.A. and Trentham,D.R. (1995) Chemotactic signal integration in bacteria. *Proc. Natl Acad. Sci. USA*, **92**, 9757–9761.

Kuo,S.C. and Koshland,D.E.,Jr (1987) Roles of *cheY* and *cheZ* gene products in controlling flagellar rotation in bacterial chemotaxis of *Escherichia coli*. *J. Bacteriol*., **169**, 1307–1314.

Kuo,S.C. and Koshland,D.E.,Jr (1989) Multiple kinetic states for the flagellar motor switch. *J. Bacteriol*., **171**, 6279–6287.

Larsen,S.H., Reader,R.W., Kort,E.N., Tso,W. and Adler,J. (1974) Change in direction of flagellar rotation is the basis of the chemotactic response in *Escherichia coli*. *Nature*, **249**, 74–77.

Levin,M.D., Morton-Firth,C.J., Abouhamad,W.N., Bourret,R.B. and Bray,D. (1998) Origins of individual swimming behavior in bacteria. *Biophys. J.*, **74**, 175–181.

Li,J., Swanson,R.V., Simon,M.I. and Weis,R.M. (1995) The response regulators CheB and CheY exhibit competitive binding to the kinase CheA. *Biochemistry*, **34**, 14626–14636.

Liu,Y., Levit,M., Lurz,R., Surette,M.G. and Stock,J.B. (1997) Receptor-mediated protein kinase activation and the mechanism of transmembrane signaling in bacterial chemotaxis. *EMBO J.*, **16**, 7231–7240.

Lowe,G., Meister,M. and Berg,H.C. (1987) Rapid rotation of flagellar bundles in swimming bacteria. *Nature*, **325**, 637–640.

Lukat,G.S., Lee,B.H., Mottonen,J.M., Stock,A.M. and Stock,J.B. (1991) Roles of highly conserved aspartate and lysine residues in the response regulator of bacterial chemotaxis. *J. Biol. Chem*., **266**, 8348–8354.

Macnab,R.M. (1995) Flagellar switch. In Hoch,J.A. and Silhavy,T.J. (eds), *Two Component Signal Transduction*. American Society for Microbiology, Washington DC, pp. 181–199.

Macnab,R.M. (1996) Flagella and motility. In Neidhardt,F.C. *et al.* (eds), *Escherichia coli and Salmonella, Cellular and Molecular Biology*. ASM press, Washington DC, pp. 123–145.

Monod,J., Wyman,J. and Changeux,J.P. (1965) On the nature of allosteric transitions: a plausible model. *J. Mol. Biol*., **12**, 88–118.

Montrone,M., Oesterhelt,D. and Marwan,W. (1996) Phosphorylation-independent bacterial chemoresponse correlate with changes in the cytoplasmic level of fumarate. *J. Bacteriol*., **178**, 6882–6887.

Ninfa,E.G., Stock,A., Mowbray,S. and Stock,J. (1991) Reconstitution of the bacterial chemotaxis signal transduction system from purified components. *J. Biol. Chem*., **266**, 9764–9770.

Ramia,M., Tullock,D.L. and Phan-Thien,N. (1993) The role of hydrodynamic interaction in the locomotion of microorganisms. *Biophys. J*., **65**, 755–778.

Sager,B.M., Sekelsky,J.J., Matsumura,P. and Adler,J. (1988) Use of a computer to assay motility in bacteria. *Anal. Biochem*., **173**, 271–277.

Segel,L.A., Goldbeter,A., Devreotes,P.N. and Knox,B.E. (1986) A mechanism for exact sensory adaptation based on receptor modification. *J. Theor. Biol*., **120**, 151–179.

Scharf,B.E., Fahrner,K.A., Turner,L. and Berg,H.C. (1998) Control of direction of flagellar rotation in bacterial chemotaxis. *Proc. Natl Acad. Sci. USA*, **95**, 201–206.

Shukla,D. and Matsumura,P. (1995) Mutations leading to altered CheA binding cluster on a face of CheY. *J. Biol. Chem*., **270**, 24414–24419.

Spiro,P.A., Parkinson,J.S. and Othmer,H. (1997) A model of excitation and adaptation in bacterial chemotaxis. *Proc. Natl Acad. Sci. USA*, **94**, 7263–7268.

Spudich,J.L. and Koshland,D.E.,Jr (1976) Non-genetic individuality: chance in the single cell. *Nature*, **262**, 467–471.

Stewart,R.C. (1997) Kinetic characterization of the phosphotransfer between CheA and CheY in the bacterial chemotaxis signal transduction pathway. *Biochemistry*, **36**, 2030–2040.

Stock,A., Koshland,D.E.,Jr and Stock,J.B. (1985) Homologies between *S.typhimurium* CheY and proteins involved in regulation of chemotaxis, membrane protein synthesis and sporulation. *Proc. Natl Acad. Sci. USA*, **82**, 7989–7993.

Stock,J.B. and Surette,M.G. (1996) Chemotaxis. In Neidhardt,F.C. *et al.* (eds), *Escherichia coli and Salmonella, Cellular and Molecular Biology*. ASM press, Washington, pp. 1103–1129.

Surette,M.G. and Stock,J.B. (1996) Role of α-helical coiled-coil interactions in receptor dimerization, signaling and adaptation during bacterial chemotaxis. *J. Biol. Chem*., **271**, 17966–17973.

Takeshita,S., Sato,M., Toba,M., Masahashi,W. and Hashimoto-Gotoh,T. (1987) High-copy-number and low-copy number plasmid vectors for lacZα-complementation and chloramphenicol- or kanamycin-resistance selection. *Gene*, **61**, 63–74.

Tawa,P. and Stewart,R.C. (1994) Kinetics of CheA autophosphorylation and dephosphorylation reactions. *Biochemistry*, **33**, 7917–7924.

Turner,L., Caplan,S.R. and Berg,H.C. (1996) Temperature induced switching of the bacterial flagellar motor. *Biophys. J*., **71**, 2227–2233.

Vigeant,M.A. and Ford,R.M. (1997) Interactions between motile *Escherichia coli* and glass in media with various ionic strengths, as observed with a three-dimensional-tracking microscope. *Appl. Environ. Microbiol*., **63**, 3474–3479.

Wang,H. and Matsumura,P. (1997) Phosphorylating and dephosphorylating protein complexes in bacterial chemotaxis. *J. Bacteriol*., **179**, 287–289.

Welch,M., Oosawa,K., Aizawa,S.I. and Eisenbach,M. (1993) Phosphorylation dependent binding of a signal molecule to the flagellar switch of bacteria. *Proc. Natl Acad. Sci. USA*, **81**, 5056–5060.

Welch,M., Oosawa,K., Aizawa,S.I. and Eisenbach,M. (1994) Effects of phosphorylation, Mg^{2+} and conformation of the chemotaxis protein CheY on its binding to the flagellar switch protein FliM. *Biochemistry*, **33**, 10270–10276.

Wolfe,A.J. and Berg,H.C. (1989) Migration of bacteria in semi solid agar. *Proc. Natl Acad. Sci. USA*, **86**, 6973–6977.

Zhao,R., Amsler,C.D., Matsumura,P. and Khan,S. (1996) FliG and FliM distribution in the *Salmonella typhimurium* cell and flagellar basal body. *J. Bacteriol*., **178**, 258–265.

Zhu,X., Amsler,C.D., Volz,K. and Matsumura,P. (1996) Tyrosine 106 of CheY plays an important role in chemotaxis signal transduction in *Escherichia coli*. *J. Bacteriol*., **178**, 4208–4215.

Received May 8, 1998; accepted June 4, 1998